Colloid Polym Sci 275:341–351 (1997)

ORIGINAL CONTRIBUTION

M. Schwab
B. Stühn

Asymmetric diblock copolymers – phase behaviour and kinetics of structure formation

Received: 12 September 1996
Accepted: 2 December 1996

M. Schwab (✉) · B. Stühn
Fakultät für Physik
Hermann-Herder-Straße 3
79104 Freiburg, Germany

Abstract The structure of a series of three molecular weights of diblock copolymers polystyrene/*b*-isoprene with 11% volume fraction of polystyrene and low polydispersity has been investigated using small angle X-ray scattering (SAXS). In between the disordered and the BCC ordered state a micellar state with liquid-like order was found. The transition between these states was investigated in a temperature-driven experiment. Whereas the micelles appear gradually with lowering temperature the formation of the BCC ordered state occurs discontinuously at a well-defined temperature. Detailed analysis of the scattering profiles provides access to the micellar size and distance in the liquid-like as well as in the BCC state. The kinetics of the ordering transition was studied using time-resolved SAXS after temperature jumps from the liquid-like to the BCC state. The growth of the micelles and their ordering on the periodic lattice were found to occur on clearly separated time scales.

Key words Block copolymers – disorder-to-order transition – micelles – BCC order – kinetics of structure formation – small angle X-ray scattering

Introduction

The phase behaviour of $[A]_n$–$[B]_m$ diblock copolymers has been of great interest for at least two decades and is still a subject of intensive research. The mostly repulsive effective interaction between the A and B segments together with the chemical bond between the A and B blocks gives rise to microphase separation and leads to a fascinating variety in the morphology. These morphologies mainly depend on the composition of the two components which is described by the volume fraction f_{vol} of block A. The so-called "classical" phases BCC – body centered cubic spheres, HPC – hexagonally packed cylinders and LAM – lamellae are well founded on theory [1, 2]. They are completed both by the recently identified bicontinuous structure with $Ia\bar{3}d$ symmetry [3], which is called the gyroid shtructure [4] and by the HPL – hexagonally perforated lamellar phase [3, 5, 6]. The OBDD – orthogonally bicontinuous double diamond is recently believed not to be an equilibrium structure [7]. For compositions of $0.2 < f < 0.8$ the thermotropic disorder-to-order (DOT) and order-to-order transitions (OOT) have been studied extensively in theory [1, 2, 7–9] and experiment [6, 10–12]. This led to a modified phase diagram [6, 7] within this range of compositions. However, little is known about the equilibrium structures for strongly asymmetric diblock copolymers. The generally expected equilibrium structures are BCC and HPC but these are not necessarily the only possible morphologies. One can also imagine spheres which form an FCC – face centered cubic, HCP – hexagonally close packed or even SC – simple cubic lattice. Sakurai and Hashimoto [13] reported an order-to-order transition for poly(styrene/isoprene) diblock copolymer

Colloid & Polymer Science, Vol. 275, No. 4 (1997)

with $f_{vol} = 0.15$. They identified a thermotropic transition from a BCC phase at lower temperatures to an HCP phase at higher temperatures. Other work [14] investigated asymmetric diblock copolymers with $f_{vol} \approx 0.25$ but focussed on the disordered state.

On the other hand, there exist only few investigations about the kinetics of structure formation for the disorder-to-order transition in bulk block copolymers [15–17, 6, 18]. In ref. [15, 16] two well separated processes were reported at a temperature jump from the homogeneously disordered to the lamellar phase in a nearly symmetric diblock copolymer ($f_{vol} = 0.44$). Similar results were obtained by other authors [17]. Other work [18] considers only the slow process to be the relevant structure formation process.

However, none of the publications mentioned above – neither the static equilibrium nor the time dependent measurements – deal with strongly asymmetric diblock copolymers. In a first part of this paper we will focus on the thermal equilibrium properties of three strongly asymmetric poly(styrene/(cis1–4)isoprene) diblock copolymers. We have used small angle X-ray scattering (SAXS) to characterize quantitatively the different morphologies of the samples and the temperature driven transition. We observed a new stable state of spherical domains with liquid-like order in between the homogeneously disordered state at high temperature and the commonly expected BCC state at low temperatures. A preliminary account of these results for one molecular weight has been given previously in [19].

We will present structural models and explicit expressions for the structure factor in the different regimes of order. The results obtained by numerical fits of model functions to the scattering data will be discussed for the full temperature range.

In the second part of this study we report the results of a series of temperature jumps from the liquid-like state of spherical domains to the BCC ordered array of spheres. The observed relaxation phenomena show at least two well separated processes.

Experimental

Sample characterization

The copolymers used in this study are polystyrene/poly(*cis*1–4)isoprene diblock copolymers with three different molecular weights. The volume fraction of polystyrene f_{vol} is about 0.1. They were synthesized anionically in our laboratory using standard high vacuum techniques. Their molecular weight distribution was determined using gel permeation chromatography and osmometry. No homopolymer fraction was found in the samples. The polysterene weight fraction was measured with proton NMR. These data are compiled in Table 1.

The trans content of the polyisoprene block was found to be about 10% from NMR measurements. In DSC measurements, all samples displayed a glass transition of the polyisoprene block. For samples 1 and 2, it was $T_g^{ls} = 211$ K. For sample 3, $T_g^{ls} = 216$ K.

Static SAXS measurements

The SAXS measurements were carried out in an evacuated Kratky compact camera to reduce background and to avoid degradation of the samples. The samples were contained in a copper sample holder with acetate windows. Temperature stability was better than 0.2 K. The source of radiation was a sealed X-ray tube with Cu anode. A graphite monochromator was applied to select the wavelength of Cu K_α radiation $\lambda = 0.1542$ nm. The accessible regime of scattering vectors in this set-up is $0.15 \leq q/\text{nm}^{-1} \leq 4$. The scattering cross-section is measured in absolute units by making use of a moving slit device (PAAR) to determine the flux of the primary beam. Data have been desmeared with respect to slit length using standard procedures [20] to result in the scattering cross-section in units of the Thomson cross-section σ_{Th}.

The registration of a scattering profile at one temperature takes approximately 120 min and the sample was annealed after each temperature changes for 30 min to make sure that it was in thermal equilibrium. Repeated heating and cooling cycles with fresh samples and varying duration were used to verify the thermal stability of the sample.

Time-resolved SAXS measurements

For the time-resolved experiments a position sensitive detector (Braun) was used. A specifically designed sample holder allows for rapid quenches with the help of cooled ethanol that is pumped through a closed circuit inside the copper block of the holder under computer control [21]. This experimental setup makes it possible to register a scattering profile in less than 30 s.

Results and discussion

The purpose of this study is to determine the structure of concentration fluctuations in strongly asymmetric diblock copolymers and to investigate the kinetics of the transition between the disordered and the ordered state. In the

Table 1 Properties of polystyrene-polyisoprene diblock copolymers used in this study

Sample No.	M_w	M_w/M_n	f	N	T_s[K]	T_{DOT} [K]	χ_h	χ_s
1	65000	1.09	0.10	810	—	≈ 445	—	—
2	46000	1.09	0.11	580	450	390	0.004(±0.002)	43(±1)
3	35000	1.07	0.12	440	≈ 220	—	0.068(±0.007)	21(±2)

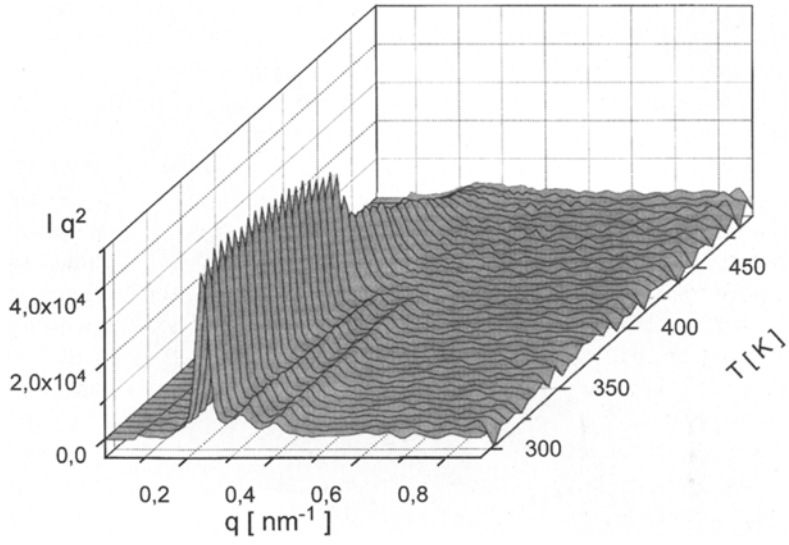

Fig. 1 SAXS pattern of sample 2 obtained during step wise heating of the sample between room temperature and 470 K. Three regimes of different degrees of order are discriminated

following we will first present and discuss the results of SAXS measurements that were obtained in thermal equilibrium. The various states of order and their dependence on temperature and molecular weight will be discussed. On the basis of these results we will then proceed to time resolved SAXS measurements following temperature jumps from the disordered into the ordered state of the block copolymer.

Equilibrium structure of diblock copolymers

In general, the state of order of a diblock copolymer melt is determined by the balance between the entropy of mixing of the two constituent monomer units and their repulsive interaction [1]. The latter is conveniently described with the product of the Flory Huggins parameter χ and the molecular weight of the polymer N. It has been shown for polystyrene/polyisoprene that χ depends strongly on temperature [14]. The system is therefore ideally suited for a study of temperature driven transitions between different states of order.

In Fig. 1 we display the results of the SAXS measurement on sample 2 in the wide temperature range between room temperature and 470 K. The temperature was raised in steps of 5 K and the sample was annealed for 30 min at each temperature before the measurement. The figure shows a scattering profile at low temperature that consists of several distinct peaks indicating the existence of a macrocrystalline structure in the sample. Raising temperature leads to a continuous, slow decrease of intensity up to 393 K. At that temperature the profile changes abruptly. The intensity of the main peak drops and the higher order reflections disappear. A broad peak remains in the profile with a shoulder at large scattering angles which becomes less prominent with increasing temperature. This measurement was repeated while cooling the sample in the same manner. Figure 2 compares the results of the heating and cooling run for the intensity I_{q^*} and the wave vector q^* of the first maximum in the scattering profile.

Above 370 K the data are reproducible within experimental error. Below this temperature, however, the intensity of the main peak in cooling exceeds the value obtained for heating. There is no clear difference between the shape of the scattering profiles in both situations. We therefore assume this intensity difference to be caused by a variation in the contrast between the polystyrene and the polyisoprene domains. The glass transition of the PS domain

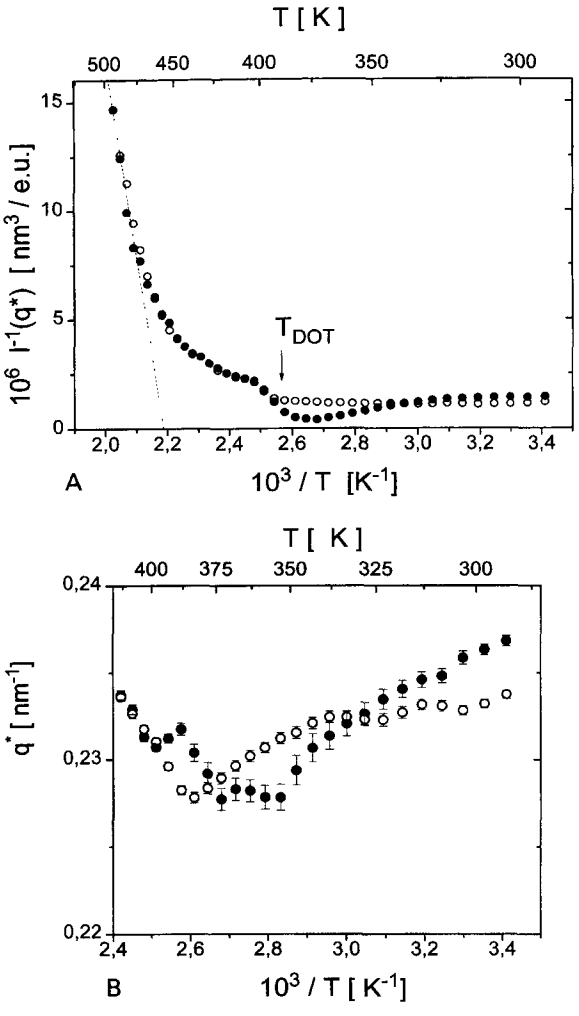

Fig. 2a The reciprocal intensity at q^* for sample 2 vs. reciprocal temperature. Mean field theory predicts a linear dependence of both quantities. At $T_{DOT} = 393$ K one finds a discontinuous increase of the intensity with lowering T ((○) heating, (●) cooling). **b** q^* is the position of the maximum in the scattering intensity profile. At the DOT it varies with temperature in accordance with the expectation for an ordering transition on a BCC lattice [8] ((○) heating, (●) cooling)

leads to a slowing down of its density increase during cooling and thus creates a large density difference between both domains as long as physical ageing has not yet taken place.

The temperature dependence of I_{q^*} in Fig. 2 also permits a precise determination of the transition temperature $T_{DOT} = 393(\pm 5)$ K. The same method has been applied earlier to the case of polystyrene/polyisoprene diblock copolymers with symmetric composition [22]. It was shown in that paper that the temperature derived in this manner coincides with the change in the power law of the dynamic shear modulus $G^*(\omega)$. Experiments of this type have been reported for a series of asymmetric diblock copolymers PS/PI [23]. It is found, however, that for a temperature interval of up to 50 K above T_{DOT} the frequency dependence of $G^*(\omega)$ did not allow a master plot construction [23, 24]. This feature was attributed to the existence of composition fluctuations in the disordered state. In the following we will give a detailed description of these fluctuations for the case of our system. The relevant temperature range is usually determined from Fig. 2 as the deviation of $I_{q^*}^{-1}(T^{-1})$ from a straight line. For the case of sample 2 this extends up to 480 K.

The linear dependence is a result of the random phase approximation (RPA) theory [1]. Within this theory the block copolymer melt becomes unstable with respect to concentration fluctuations at a spinodal temperature T_s. T_s is extrapolated from the high temperature data for I_{q^*} as is shown in Fig. 2a as the dotted line. The resulting T_s values are included in Table 1. However, care must be taken in the interpretation of this parameter as it is influenced by concentration fluctuations [22].

A further interesting observation is made in Fig. 2b concerning the position q^* of the first maximum in the scattering profile. As opposed to the assumption of the early RPA theory [1] this wave vector depends clearly on temperature. Within the disordered state the shift of q^* to smaller values with increasing interaction, i.e., lowering temperature, was attributed to a stretching of the polymer coil [14]. This trend is reversed, however, when the transition to the ordered state takes place. This signature is expected theoretically for a transition into a BCC lattice [8, 9].

We now turn to a detailed discussion of the three different types of scattering profiles that are discernible in Fig. 1 with variation of temperature. For the sake of clarity we will mainly focus on the results obtained from sample 2 as it is the one displaying all three structures in the accessible temperature range. At high temperature we find a broad peak in the scattering profile of sample 2. The same type of scattering is obtained from sample 3 in the full range of temperatures. As an example we show in Fig. 3 the result for sample 2 at $T = 458$ K. The full curve in the figure represents a fit of Leibler's RPA theory [1]. The polydispersity of the polymer has been taken into account using the method outlined in ref. [14]. The fit obviously describes the data very well and allows us to extract the value of the interaction parameter χN from the data. The broken line in Fig. 3 indicates the contribution of density fluctuations to the scattering which is given as

$$I_\kappa = \langle \eta \rangle^2 k_B T \kappa_T \,, \tag{1}$$

where $\langle \eta \rangle$ is the mean electron density of the sample and κ_T the isothermal compressibility. It has been shown earlier [14] that Eq. (1) indeed describes this scattering

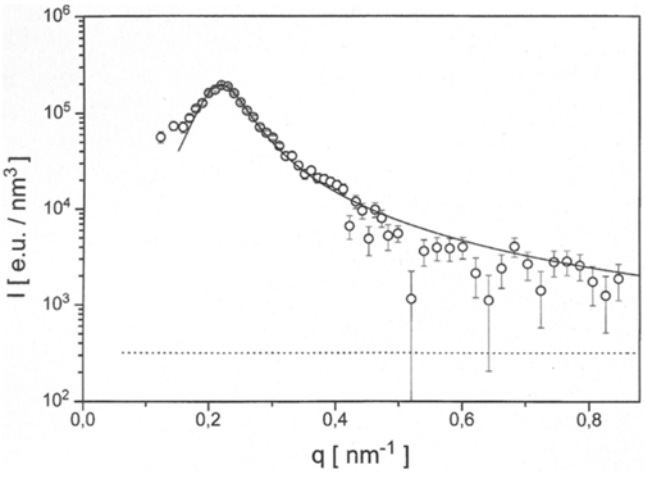

Fig. 3 The SAXS pattern from sample 2 at $T = 458$ K is characteristic of the disordered state of the diblock copolymer. It is well described by mean field theory [1] if polydispersity is taken into account [14] (full curve). The broken line shows the contribution of density fluctuations to the scattering

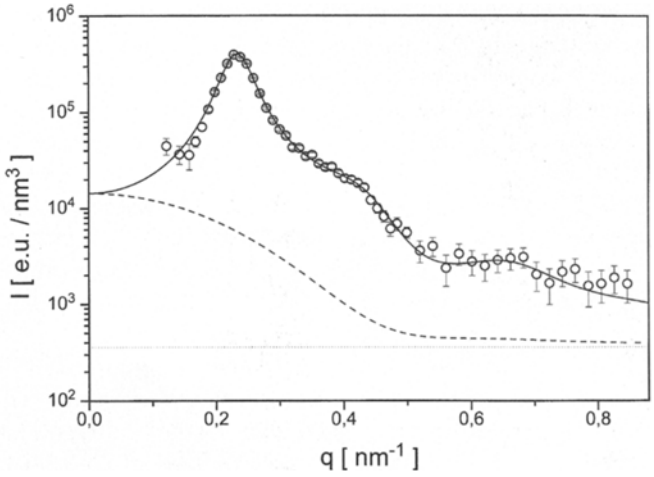

Fig. 4 Example of the SAXS pattern from sample 2 at $T = 413$ K in the micellar regime. The full curve is a fit of the hard sphere model of Eq. (3). The broken line shows the square of the form factor of single spheres without interference and the dotted line is the q independent background (see Eq. (1))

contribution quantitatively. In order to compare the χN values with results from other sources we use a mean molar volume to calculate the effective number of segments N (see Table 1). We then find the interaction parameter χ for the data refering to the high temperature regime of Fig. 1 to be linearly dependent on reciprocal temperature $\chi = \chi_s + \chi_h/T$. The parameters χ_s and χ_h, differ for samples 2 and 3 (see Table 1). However, compared to the results of ref. [14], there is no systematic dependence on molecular weight. Whereas the general form for the temperature dependence of χ is confirmed by our results and by other experimental methods [23]: the parameter χ_h is found to vary widely. The cause for these discrepancies may be different in the various experimental methods applied. In the case of the scattering experiment on a diblock copolymer in its disordered state, the main source of error will be concentration fluctuations. Their effect is a temperature dependent reduction of the apparent interaction parameter with respect to its bare value [2].

At lower temperatures the scattering profile from the diblock copolymers changes in two respects. The most prominent feature is the increase in the intensity of the main scattering maximum at q^* as shown in Fig. 2. Close inspection of the curve, however, reveals the development of a shoulder in the profile at larger q. This is in contrast to the temperature induced changes of the scattering profile from symmetric diblock copolymers. It reflects the existence of well-defined concentration fluctuations in the sample. In Fig. 4 we show data obtained at $T = 413$ K. Besides the main peak at $q = 0.22\ \mathrm{nm}^{-1}$ one observes two further maxima at larger q. The peaks are still rather broad and less intense than the reflections found at even lower temperatures (see below).

This form of the scattering profile may be understood in the framework of a micelle model [9]. As a consequence of the increasing repulsive interaction between polystyrene and polyisoprene blocks with lowering temperature the system forms micelles consisting of a polystyrene core and a polyisoprene cover. Not all chains are packed into this structure. A fraction of free block copolymer chains forms a continuous matrix in between the micelles. In order to describe our data quantitatively we need to calculate the form factor of the micelles as well as the pair correlation functions between micelles. The main part of the scattering contrast will be between the polystyrene core and the matrix. We can therefore use the well-known form factor of a sphere with R_{sp} denoting the radius of the polystyrene core: [25]

$$\Phi(q) = 3v_{sp}\frac{\sin(R_{sp}q) - R_{sp}q\cos(R_{sp}q)}{(R_{sp}q)^3}, \tag{2}$$

where v_{sp} is the volume of a sphere. The scattering intensity for a dilute system of spheres would then be given as the square of $\Phi(q)$. Within this simple approach, however, we cannot describe our data. The interference between different spheres contributes significantly to the scattering pattern and we need to take this into account.

A closed form of a pair correlation function has been derived for a liquid consisting of hard spheres [26, 27]. This model introduces two more parameters describing the range of the interaction between micelles as an effective

hard sphere radius R_{hs} and the volume fraction of spheres η. This correlation function has been applied earlier to block copolymer/homopolymer blends [28]. The parameter R_{hs} for the present case will be expected to be larger than the core radius R_{sp}. It is of the order of the full size of the micelle.

The scattered intensity is given as the product of the square of the single particle form factor and the interference factor $S(q, R_{hs}, \eta)$, which is the Fourier transform of the pair correlation function

$$I(q) = K\bar{\Phi}^2(q)S(q, R, \eta) . \tag{3}$$

The prefactor K depends on the scattering contrast between the polystyrene sphere and the matrix. The spherical form factor needs to be averaged over the size distribution $g(R)$ of the micelle cores. This average is denoted by the horizontal bar in Eq. (3). The functional form of $g(R)$ is assumed to be a Gaussian with a mean value $\bar{R} = R_{sp}$ and a second moment $\sigma^2 = \overline{(R - \bar{R})^2}$

$$g(R) = \frac{1}{\sqrt{2\pi}\sigma} \exp\left(-\frac{1}{2} \left(\frac{R - \bar{R}}{\sigma} \right)^2 \right) . \tag{4}$$

We note that Eq. (4) clearly becomes unphysical as soon as σ increases such that negative values of R contribute significantly to the average. In this situation a more suitable mathematical form for $g(R)$ is the Schulz distribution. In the present situation it turns out that $\sigma/R_{sp} < 0.2$ in all cases such that the use of the Gaussian distribution is justified.

The interparticle interference then results in a structure factor

$$S(q, R_{hs}, \eta) = \frac{1}{1 + 24\eta(G(A)/A)} \tag{5}$$

with $A = 2qR_{hs}$ and

$$\begin{aligned} G(A) = {} & \frac{\alpha}{A^2}(\sin A - A\cos A) + \frac{\beta}{A^3}(2A\sin A \\ & + (2 - A^2)\cos A - 2) \\ & + \frac{\gamma}{A^5}\{ - A^4\cos A + 4[(3A^2 - 6)\cos A \\ & + (A^3 - 6A)\sin A + 6]\} . \end{aligned} \tag{6}$$

The model of micelles with a liquid-like order provides a quantitative fit of our data in the full range of temperatures between T_{DOT} and 450 K. As an example we display the data obtained from sample 2 at $T = 413$ K in Fig. 4. The full curve is a fit of Eq. (3). The model reproduces the first maximum as well as the maxima at larger q. In order to demonstrate the effect of the spherical form factor we plot $K\bar{\Phi}^2(q)$ as the broken line in Fig. 4. The q-independent scattering contribution is again caused by the density fluctuations in the sample. It is of negligible influence in the range of the interparticle interference peak but needs to be taken into account at large q.

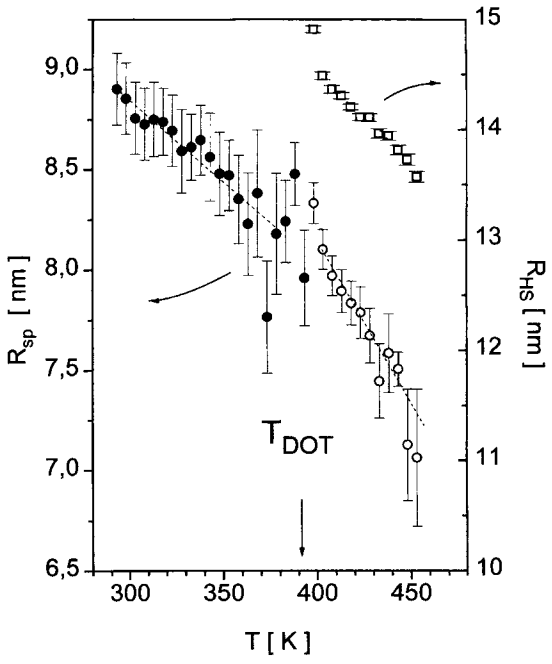

Fig. 5 Temperature dependence of the polystyrene domain radius R_{sp} (left axis) and the hard sphere radius R_{HS} (right axis). Open symbols are obtained within the model of liquid like order between micelles (Eq. (3)). Filled symbols are results of a fit of the BCC model (Eq. (12))

The picture resulting from the evaluation of the scattering profiles is a system consisting of spherical micelles in a matrix comprising a certain fraction of diblock copolymer molecules that are still in their disordered state. In view of the finite though small polydispersity of the samples one may expect that the low molecular weight will primarily remain in the matrix. Polydispersity may thus be seen to stabilize the existence of the micellar state with liquid-like order. We emphasize that the significance of the hard sphere radius R_{hs} is merely that of a model parameter which captures the main features of the inter-micelle interaction. A more realistic interaction potential is derived in ref. [29].

We now proceed to investigate the temperature dependence of the various parameters that characterize this type of liquid-like order between micelles. In Fig. 5 we display the results for the radius of the polystyrene domain for sample 2 in the temperature regime that shows the liquid-like order between micelles. They are reproducibly obtained in heating and cooling. We find the radius of the domains to increase significantly with lowering

temperature by 18%. This increase can be attributed only partially to a sharpening of the interphase between the polystyrene core and the polyisoprene as the average distance between the spheres also grows (see below). The increase is therefore mainly caused by the successive implementation of polystyrene blocks into the domains. At the lowest temperature the domain radius is $R_{sp}(398\ K) = 8$ nm. This results in 270 molecules being packed into one micelle. The smallest observable micelle has $R_{sp}(450\ K) = 7.2$ nm. The radius of the polystyrene domain is to be compared to the unperturbed end-to-end distance of the polystyrene block $R_{ee} = 4.7$ nm which means that the polystyrene block is highly extended. The stretching is estimated in ref. [29] for the highest temperature at which the first micelle is formed:

$$R_{sp} = 0.89\,\alpha_c^{1/6}\,R_{ee}\,, \tag{7}$$

where α_c is determined from the implicit equation $\alpha_c = \ln(1/f) + 1/2\ln\alpha_c + 2.06\,\alpha_c^{(1/6)}$ which for our composition $f \approx 0.11$ has the solution $\alpha_c = 7.16$. We would therefore expect a smallest value for the polystyrene domain radius of 5.8 nm. The data shown in Fig. 5 are significantly larger than this threshold value.

A qualitatively similar behavior is found in the temperature dependence of the range of the interaction potential between the micelles as described by the hard sphere radius R_{hs}. Figure 5 compares these results with the radius of the polystyrene domains. The relative increase of R_{hs} with lowering T is smaller than that of the domain radius. Finally we can combine the results for the volume fraction of hard spheres η, the hard sphere radius R_{hs} and the polystyrene domain radius R_{sp} to calculate the volume fraction f_{sp} of polystyrene accumulated in the micellar cores for a given temperature:

$$f_{sp} = \eta\left(\frac{R_{sp}}{R_{hs}}\right)^3\,, \tag{8}$$

where f_{sp} would be expected to approximate the overall volume fraction of polystyrene f at low temperatures as soon as all diblock copolymer chains are organized in the micelles. The data shown in Fig. 6 indeed display this behavior. At $T = 398$ K about 8% of the volume is filled with polystyrene spheres which means that a large fraction of the chains are connected to micelles. However, f_{sp} continues to increase also below the ordering transition as will be discussed below.

Finally we observe that the size distribution of the polystyrene domains remains nearly constant within the investigated temperature range. It is well described by a Gaussian distribution of radii (cf. Eq. (4)) with $\sigma = 1.5$ nm. Raising temperature leads to a homogeneous decrease of the micelle size and to a release of polymer chains into the matrix.

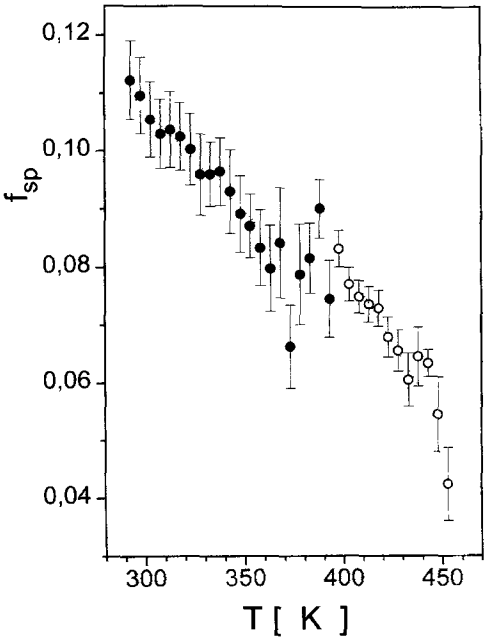

Fig. 6 Volume fraction of polystyrene blocks organized in micellar cores. The open symbols are derived from Eq. (8) and the filled symbols from Eq. (13)

We now turn to the structure found below the phase transition which for sample 2 is located at $T_{DOT} = 393(\pm 5)$ K and for sample 1 at $T_{DOT} = 448(\pm 5)$ K. The scattering profile changes abruptly at this temperature as is observed in Fig. 1. We remark that the discontinuous nature of the transition may easily be overlooked in the experiment, if the sample is not given sufficient time to relax into its equilibrium at each temperature. We will return to this point in the subsequent section. In Fig. 7 we now show in more detail a representative profile for the ordered state of samples 1 and 2. Besides the main peak at q^* the SAXS pattern shows at least two higher orders at positions $\sqrt{2}q^*$ and $\sqrt{3}q^*$. The width of these peaks is significantly smaller than that of the main peak in the micellar phase at elevated temperature. Moreover, the pattern is characterized by a diffuse scattering component which depends markedly on the scattering vector q and gives rise to the broad shoulder around $q \approx 0.6\ nm^{-1}$ in Fig. 7.

The transition at T_{DOT} has obviously led to a macrocrystalline state in which the micelles are located at well-defined periodic lattice positions. The sequence of peak positions is in accordance with a BCC structure as is expected for this composition. Our aim now is to arrive at a quantitative description of the scattering pattern in terms

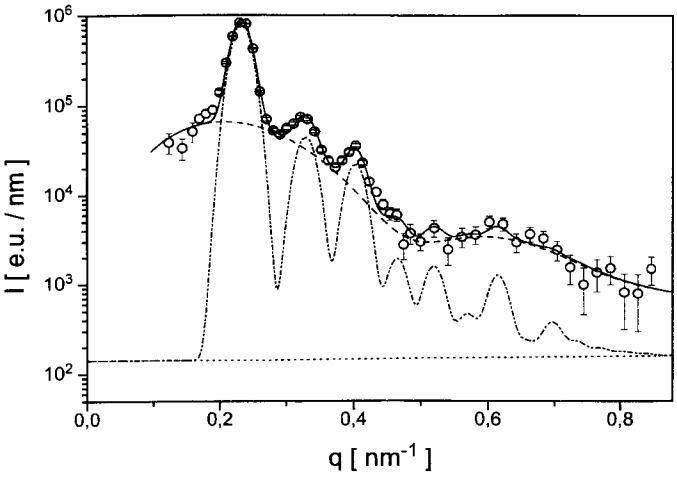

Fig. 7 Typical SAXS pattern of the ordered state of samples 1 and 2. The data are from sample 2 at $T = 318$ K. The full curve is a fit of the BCC model (see Eq. (12)). The broken lines indicate the Bragg and diffuse component, respectively. The q-independent dotted line is the scattering contribution from density fluctuations

Table 2 List of allowed reflections for a BCC lattice. (space group $Im\bar{3}m$). (hkl) are the Miller indices and n_{hkl} denotes the multiplicity of a reflection

h	k	l	n_{hkl}
1	1	0	12
2	0	0	6
2	1	1	24
2	2	0	12
3	1	0	24
2	2	2	8
3	2	1	48
4	0	0	6
3	3	0	12
4	1	1	24
4	2	0	24
3	3	2	24
4	2	2	24
5	1	0	24

of this structural model and to obtain information on the details of the structure such as micellar size. We therefore use a refinement method that is commonly applied in the study of polycrystalline powder patterns in crystallography but apply it to the small angle scattering regime. The scattering intensity consists of two components: a Bragg component I_{hkl} caused by the regular periodic order and a diffuse component I_{diff} which is due to positional disorder of the micelles.

I_{Bragg} is simply given as the sum of Bragg peaks at positions described by the Miller indices (hkl). For a cubic lattice the peak positions are given in terms of the lattice constant a as

$$q_{hkl} = \frac{2\pi}{a}\sqrt{h^2 + k^2 + l^2}\,. \tag{9}$$

Their intensity is given by the average form factor of the polystyrene domain at the wave vector position q_{hkl}, $\bar{\Phi}^2(q_{hkl})$, and the multiplicity n_{hkl} of the reflection $\{hkl\}$:

$$I_{\text{Bragg}}(q) = K_{\text{Bragg}}\bar{\Phi}^2(q_{hkl})\frac{n_{hkl}}{q^2}G_{hkl}(q, q_{hkl}, \sigma_{\text{Bragg}}) \times \exp(-q^2u^2/3)\,, \tag{10}$$

where $G_{hkl}(q, q_{hkl}, \sigma_{\text{Bragg}})$ denotes a normalized Gaussian at position q_{hkl} with a variance σ_{Bragg} which is the same for all reflections. The intensity is further modified by the Lorentz factor which for the present case is $1/q^2$. The intensity of the Bragg reflections is decreased by the existence of disorder which is here described by a Debye–Waller factor with a mean-squared displacement of the micelles from their lattice positions u^2.

The finite width of the interface between the polystyrene domain and polyisoprene gives rise to a factor of the same form as the Debye–Waller factor in Eq. (10). It cannot be discriminated from the disorder on the basis of our data and u^2 therefore describes both effects.

Equation (10) contains as variable parameters a prefactor K_{Bragg}, the lattice constant a, the radius of the polystyrene domain R_{sp}, and the mean-squared displacement u^2. In the refinement procedure we include all allowed reflections in the q range under consideration. A list of the reflections is given as Table 2.

The scattering unit in this macrocrystal is the polystyrene domain which as opposed to atomic scatterers is rather large. Consequently, the diffuse scattering part carries the wave vector dependence of the form factor. A similar situation is encountered in the scattering from oligomeric crystals [30]. If we assume the deviation of the local form factor of a micelle to be uncorrelated then

$$I_{\text{diff}} \propto (1 - \exp(-q^2u^2/3))\bar{\Phi}^2 + (\overline{\Phi^2} - \bar{\Phi}^2)\,. \tag{11}$$

In order to simplify calculations we observe that averaging Φ with respect to the size distribution will smear out its maxima and we assume $I_{\text{diff}} \approx K_{\text{diff}}(1 - \exp(-q^2u^2/3))\overline{\Phi^2}$, with K_{diff} an adjustable prefactor. The radius of the polystyrene spheres enters the expressions for the intensities of the Bragg reflections as well as the q-dependence of diffuse scattering.

A third contribution to the scattering I_κ arises from the density fluctuations and is taken into account as a constant. The scattered intensity is then given as

$$I(q) = I_{\text{Bragg}} + I_{\text{diff}} + I_\kappa\,. \tag{12}$$

The data in Fig. 7 are shown together with a fit of Eq. (12) as a full curve. The assumption of a BCC structure

consisting of spherical micelles obviously provides a very good description of the data. As a first result of the refinement we obtain the temperature dependence of the lattice constant a as derived from a fit of Eq. (12) to the data in the temperature range from room temperature to 393 K. With the exception of the immediate vicinity of the transition temperature the lattice constant and therefore the distance between micelles is decreasing with lowering temperature. This variation is of course already visible in the variation of q^* as shown in Fig. 2b. It is in accordance with theoretical expectation for ordering on a BCC lattice [8].

Heating and cooling runs do not superimpose in this temperature range. The glass transition of the polystyrene domains obviously causes the ordering to be very slow. The change of a with temperature is considerably larger than would be expected on the basis of the thermal expansion of polyisoprene. Moreover this decrease of the distance between micelles is accompanied by an increase of the radius of the polystyrene domain as shown in Fig. 5. The data for $T \leq T_{DOT}$ are derived from the fit of Eq. (12) whereas for $T > T_{DOT}$ we apply the model formulated by Eq. (5). The radius R_{sp} is found to vary continuously with T which supports the applicability of our structural models. Below T_{DOT} the rate of increase with lowering temperature is smaller than above but the micelles continue to grow. The observed shrinking of the lattice must therefore be entirely due to changes in the polyisoprene matrix.

We can again calculate the volume fraction of polystyrene spheres f_{sp} as was done before for the temperature regime above T_{DOT} (see Eq. (8)):

$$f_{sp} = \frac{8\pi}{3}\left(\frac{R_{sp}}{a}\right)^3 . \tag{13}$$

These data are included in Fig. 6. They continuously match the results from the liquid like ordered state thus supporting the applicability of both structural models. As was noted above the overall volume fraction of polystyrene is approached around room temperature.

Kinetics of the ordering transition

Having established the different states of order for the asymmetric diblock copolymers as a function of temperature we now turn to the question of the kinetics of ordering. As was mentioned above the formation of order at the disorder-to-order transition is a slow process and long annealing times are required to prepare the system in its thermal equilibrium. On the other hand, this opens the way for a real time experiment in which we observe the change of the structure factor with time after a quench from the disordered state into the BCC ordered state below T_{DOT}. Such experiments have been reported earlier for the case of symmetric diblock copolymers of polystyrene and polyisoprene [31, 32, 17]. However, the situation for a symmetric diblock is special as the ordering process is essentially one dimensional [33]. In the present situation we have a transition leading from a liquid consisting of spherical micelles to a three dimensionally ordered, BCC type structure.

In the following we present the results from a series of quench experiments using sample 2 for which the ordering transition occurs at an experimentally convenient temperature. The sample is prepared in its micellar state at $T = 413$ K and then quenched to three temperatures below T_{DOT}. In separate measurements we have monitored the temperature at the location of the sample and determined the time to reach the end temperature to be smaller than 30 s. After that time, temperature fluctuations are smaller than 3 K and smaller than 0.5 K after 150 s.

In Fig. 8 we show the results of the time-resolved SAXS measurement following a quench 413 K → 343 K. The first 10 scattering profiles were taken during time intervals of 30 s. For the subsequent measurements the time intervals were continuously increased. We were thus able to extend the measurement for up to 20 h. We observe a slow built-up of intensity after 2×10^4 s which is accompanied by the development of second and third order reflections. In order to analyze the change of structure with time in more detail we fit the first order reflection with a Gaussian and determine the time dependence of the intensity, the full width at half maximum FWHM, and the scattering vector position q^*. The result of this analysis is depicted in Figs. 8(a)–(c).

Immediately after the temperature jump the intensity of the peak increases over its equilibrium value at the starting temperature. The characteristic time for this increase is $\tau_1 = 120(\pm 20)$ s and therefore significantly larger than the time for the variation of temperature itself. The full curve in Fig. 8 represents fits of an exponential increase (or decrease, respectively) of the parameter. This rapid change of peak intensity has also been observed in the case of the lamellar diblock copolymers. Its origin is in both cases the progress in the separation of the styrene and isoprene parts giving rise to improved scattering contrast and consequently increased intensity. In the present case we know from the investigation of the equilibrium structure that a significant part of the diblock copolymers are not bound to micelles at the starting temperature (see Fig. 6). The ordering process must therefore involve as a first step the incorporation of these chains into the micelles and consequently the increase of the polystyrene domain size (Fig. 5).

Our data show that the ordering onto the BCC lattice does not occur at the same time. This formation of

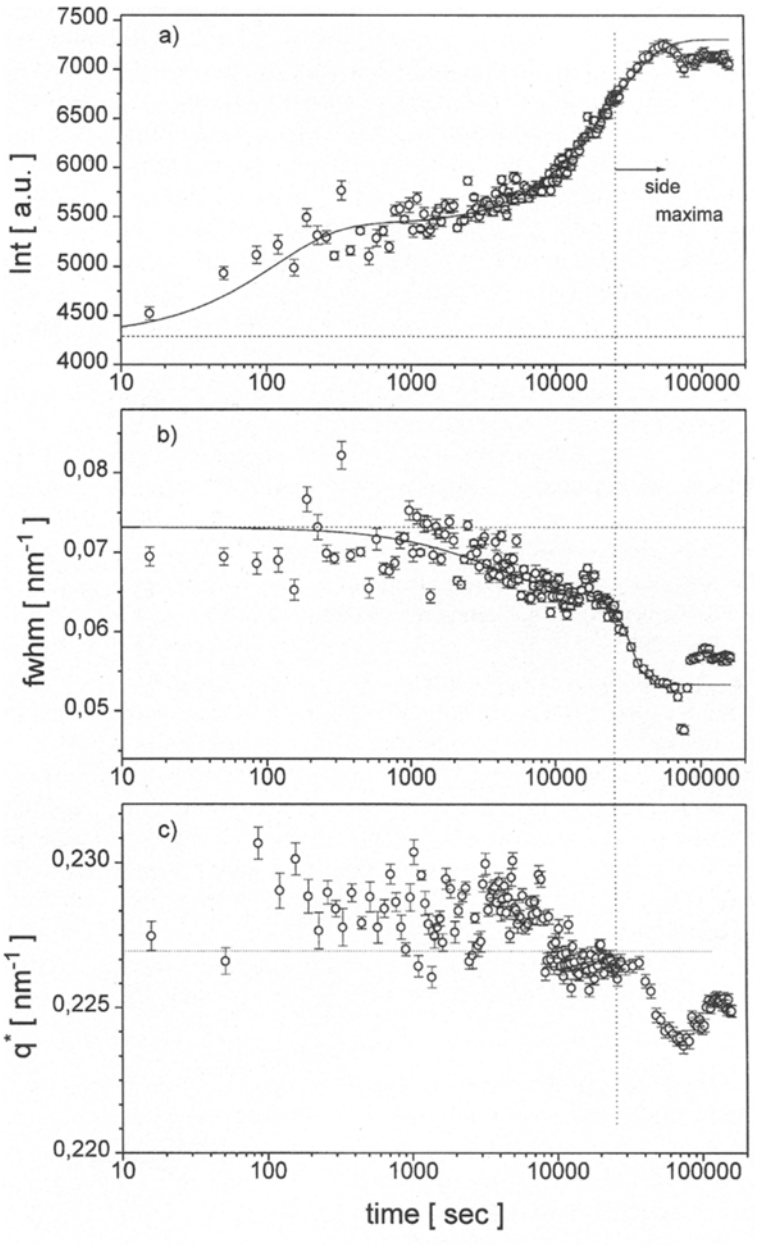

Fig. 8 Variation of the first order maximum with time following a temperature jump 413 K → 343 K. The peak is fitted with a Gaussian. Two time scales are found for the variation of the peak parameters. The vertical line marks the onset of the higher order reflections. The initial value of the peak parameters at $t = 0$ are included as dotted lines. (a) Integral peak intensity: increase on both time scales. (b) FWHM: significant decrease on slow time scale. (c) q^*: shift to smaller values on slow time scale

long-range order is displayed in two properties of the scattering profile. The first is the decrease in the FWHM of the first maximum as a result of the enlarged correlation length. The second is the existence of high order reflections. The onset of these maxima is depicted as a vertical dotted line in Fig. 8. In parallel with the sharpening of the peak Fig. 8(c) shows a shift of its wave vector q^* to smaller values. We find this shift in the same manner for a quench temperature of 363 K but not for the highest value of 383 K. In the latter case the shift in q^* occurs before the high order reflections are visible and the FWHM decays. q^* obviously is influenced by a stretching of the polymer chains as well as by the ordering of the micelles on the lattice and our experimental resolution may not be sufficient to discriminate between both effects.

At very long times the data in Fig. 8 show a decrease in the peak intensity which is accompanied by a reverse shift in q^*. This is a reproducible effect which could be caused by a transition between two distinct lattice types. However, we were unable to identify these differences in the scattering profiles as the resolution of the position sensitive detector used in the kinetic study is too small.

Conclusions

In the investigation of the equilibrium structure of strongly asymmetric diblock copolymers of polystyrene–b-polyisoprene we have identified three different states of order. In between the disordered state at high temperature or low molecular weight and the BCC ordered state at low temperature a micellar state with liquid-like order has been found. The size of the micelles depends strongly on temperature. The ordering onto the BCC lattice could be observed as a temperature driven phenomenon. In time-resolved SAXS experiments, after the temperature jumps from the micellar into the BCC state it was shown that the ordering process consists mainly of two distinct stages which are identified as an increase of the micelles due to the incorporation of more molecules from the matrix and a subsequent ordering onto the periodic lattice.

Due to the limited resolution of the experiment it was not possible to clearly identify the transition between differently packed periodic states which is suggested to occur at long annealing times.

References

1. Leibler L (1980) Macromolecules 13: 1602
2. Fredrickson G, Helfand E (1987) J Chem Phys 87:697
3. Förster S, Khandour AK, Zhao J, Bates FS, Hamley IA, Ryan AJ, Bras W (1994) Macromolecules 27:6922
4. Hajduk DA, Harper PE, Gruner SM, Honecker CC, Kim G, Thomas EL, Fetters LJ (1994) Macromolecules 27:4063
5. Hamley IW, Koppi DA, Rosedale JH, Bates FS, Almdal K, Mortensen K (1993) Macromolecules 26:5959
6. Khandpur A (1995) Macromolecules 28: 8796
7. Matsen MW, Bates FS (1996) Macromolecules 29:1091
8. Olvera de la Cruz M (1991) Phys Rev Lett 67:85
9. Semenov AN (1989) Macromolecules 22: 2849
10. Kasten H, Stühn B (1995) Macromolecules 28:4777
11. Ogawa T, Sakamoto N, Hashimoto T, Han CD, 'Baek DM (1996) Macromolecules 29:2113
12. Winey KI, Gobran DA, Xu Z, Fetters LJ, Thomas EL (1994) Macromolecules 27:2392
13. Sakurai S, Kawada H, Hashimoto T (1993) Macromolecules 26:5796
14. Holzer B, Lehmann A, Stühn B, Kowalski M (1991) Polymer 11:1935
15. Schuler M, Stühn B (1993) Macromolecules 26:112
16. Stühn B, Vilesov A, Zachmann HG (1994) Macromolecules 27:3560
17. Floudas G, Pakula T, Fischer EW, Hadjichristidis N, Pispas S (1994) Acta Polymer 45:176
18. Hashimoto T, Sakamoto N (1995) Macromolecules 28:4779
19. Schwab M, Stühn B (1996) Phys Rev Lett 76(6):924
20. Strobl G (1970) Acta Cryst A26:367
21. Schwab M (1995) Thesis, Universität Freiburg
22. Stühn B, Mutter R, Albrecht T (1992) Europhys Lett 18:427
23. LaMonte Adams J, Graessley W, Register R (1994) Macromolecules 27:6026
24. Bates F, Rosedale J, Fredrickson G (1990) J Chem Phys 92:6255
25. Guinier A (1963) X-Ray Diffraction. Freeman, San Francisco
26. Wertheim M (1963) Phys Rev Letters 10:321
27. Thiele E (1963) J Chem Phys 39:474
28. Kinning D, Thomas E (1984) Macromolecules 17:1712
29. Semenov AN (1985) Sov Phys JETP 61:733
30. Albrecht T, Elben H, Jaeger R, Kimmig M, Steiner R, Strobl G, Stühn B, Schwickert H, Ritter C (1991) J Chem Phys 95:2807
31. Schuler M, Stühn B (1993) Macromolecules 26:112
32. Stühn B, Vilesov A, Zachmann H (1994) Macromolecules 27:3560
33. Vakulenko S, Vilesov A, Stühn B, Frenkel S (1996) J Chem Phys, in press